Stress-strain Constitutive Models Along the Grain of Original Bamboo Based on Classification

Zhili Cui,[a,*] Zhenhua Jiao,[b] Wei Tong,[a] and Pan Li [a]

To establish the constitutive model of original bamboo, the tensile and compressive tests along the grain of original bamboo were investigated. The original bamboo was graded according to the elastic modulus, and a stress-strain constitutive model of original bamboo was proposed. The results of the study show that the tensile failure mode of original bamboo along the grain is brittle failure, and the compression along the grain is ductile failure. The bamboo was divided into three grades I, II, and III, and the proportion of II and II was more than 80%. A linear constitutive model was used for tension along the grain of original bamboo, a "three-fold" model was used for simplified constitutive model for compression along the grain, and the Sargin model was used for accurate constitutive model. The classification method proposed in this paper can result in the efficient utilization of bamboo resources, and the proposed constitutive model can promote the analysis and engineering application of original bamboo architecture.

DOI: 10.15376/biores.19.2.3031-3046

Keywords: Phyllostachys edulis bamboo; Grade; Performance index; Constitutive relationship

*Contact information: a: Anhui University of Science & Technology, School of Mechanics and Photoelectric Physics, Huai Nan 232001, China; b: Anhui University of Science & Technology, Key state laboratories, Huai Nan, 232001, China; *Corresponding author: zhlcui@aust.edu.cn*

INTRODUCTION

The Chinese government has increasingly attached importance to high-quality economic development, and at the same time it has become more conscious of ecological environment protection. It has proposed the goal of carbon peak by 2030 and carbon neutral by 2060. To achieve the goal of carbon peak and carbon neutral, it is essential to innovate contemporary architecture, which requires the transformation of traditional buildings into green buildings. Bamboo, known as "plant steel bar", is an ideal building material (Tian *et al.* 2018; Li *et al.* 2020). Bamboo has many advantages (Chen *et al.* 2012; Chen *et al.* 2018; Skuratov *et al.* 2021). It is the fastest growing plant in the world, and its growth cycle is shorter than wood. Bamboo has high strength, as well as good elasticity and toughness. The design and construction of the bamboo building is flexible and can extend the life of the building by replacing damaged parts. Bamboo buildings are comfortable and pleasant to the eye. Driven by the government and international organizations and combined with modern advanced construction technology, bamboo architecture has broad application prospects (Huang *et al.* 2017; Masood *et al.* 2017; Nurazka *et al.* 2021; Zhou *et al.* 2023).

Up to this point, research on original bamboo has focused mainly on microstructure and chemical composition (Lo *et al.* 2008; Jiang *et al.* 2015; Liu and Zhou *et al.* 2021), basic physical and mechanical properties (Mitch *et al.* 2010; Liu *et al.* 2014; Zhou *et al.* 2022), prediction of mechanical properties (Liu *et al.* 2021a; Liu *et al.* 2021b), production

technology (Li *et al.* 2016; Ni *et al.* 2016), testing and theoretical analysis of composite components (Fang *et al.* 2015; Li *et al.* 2015; Made *et al.* 2016; Zhao *et al.* 2017; Wang *et al.* 2021), *etc*. Bamboo mainly consists of vascular bundles and basic tissues. Vascular bundle is responsible for carrying load, and the basic organization is responsible for load transfer (Lo *et al.* 2008). Bamboo contains a large amount of cellulose (40 to 60%), hemicellulose, and lignin, as well as starch, protein, and other chemical components (Jiang *et al.* 2015). The diameter of bamboo gradually decreases with height, whereas the strength generally increases with the height of bamboo stalk (Liu *et al.* 2021b), and gradually increases from the inside to the outside of bamboo wall (Liu *et al.* 2014). The strength of bamboo along the grain direction is significantly higher than that of the horizontal grain direction (Mitch *et al.* 2010). Liu *et al.* (2021c) carried out a systematic experiment on the physical and mechanical properties of original bamboo. They obtained mechanical properties such as compressive strength and elastic modulus along the grain, tensile strength and modulus along the grain, flexural strength and elastic modulus, *etc*. The relationship between the above-mentioned mechanical properties and wall thickness and perimeter was analyzed, and the prediction formulas for various mechanical properties, wall thickness, and perimeter were put forward. By such an approach, the relationship between the mechanical properties of raw bamboo was established. In order to make bamboo more convenient to be used in building structures, standardized bamboo composite materials are produced by reorganizing original bamboo, impregnating bamboo, and heat curing under high temperature and high pressure (Li *et al.* 2016; Ni *et al.* 2016). To study the mechanical properties of standardized bamboo composite members, Li *et al.* (2015) conducted the axial compression test and theoretical analysis of laminated bamboo column. The results showed that laminated bamboo column had good mechanical properties. Fang *et al*. (2015) developed a new type of GFRP-bamboo-wood laminated sandwich beam and studied its mechanical properties. The results show that increasing the thickness of bamboo layer and GFRP layer plays an important role in improving the flexural stiffness and ultimate load of sandwich beam.

In order to promote finite element analysis of bamboo structure, the establishment of a constitutive model is very important. Li *et al.* (2020) carried out experiments on bamboo scrimber and studied its constitutive relationship. They proposed three stress-strain relationship models including a quadrilinear model, a quadratic function model, and a cubic function model. The latter two models can better predict the stress-strain relationship in the elastic-plastic stage. Wei *et al.* (2020) explored the tensile and compressive failure modes of glulam bamboo along the grain and fitted its stress-strain constitutive model with the Richard-Abbott model. However, the constitutive model of original bamboo is still lacking. In order to promote the application of original bamboo structure, it is urgent to put forward the constitutive model of original bamboo. Different from standardized materials such as recombinant bamboo and glulam bamboo, the mechanical properties of original bamboo have great variability, so the culms must be graded before studying the constitutive model of original bamboo. Classification can effectively improve the utilization value of original bamboo resources.

In order to classify bamboo and establish a constitutive model, tensile and compressive tests were used to analyze the failure modes of tensile and compressive specimens along the grain. The bamboo was classified. A stress-strain constitutive model of original bamboo material was proposed. The research results of this paper will promote the finite element analysis and engineering application of original bamboo structures.

EXPERIMENTAL

Materials

The original bamboo studied in this paper is *P. edulis* bamboo produced in China. The bamboo was 4 years old. The wall thickness of bamboo stalks was not less than 6 mm. In the bamboo forest, the original bamboo without cracking, mildew, corrosion, or moth - eaten condition was randomly selected for cutting. In order to prevent bamboo culm from cracking during felling, the felling position is chosen close to the bamboo node. After cutting, the samples were air dried, and the tensile and compressive specimens along the grain were made. The distribution of specimens in the bamboo culm achieved uniform distribution of tensile and compressive specimens along the bamboo culm. Referring to the standards JG/T199-2007 (2007) and ISO 22157-1-2019 (2019), a total of 100 tensile specimens and 200 compressive specimens along the grain were prepared. Before loading, the height (*h*), wall thickness (*t*) and diameter (*D*) of the specimen were recorded. After loading failure, a small specimen with a size of 20 mm × 20 mm × *t* mm was intercepted near the failure of the specimen for density measurement.

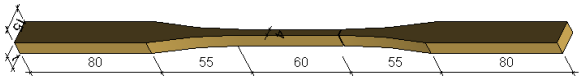

(a) UT specimen size

(b) UT test

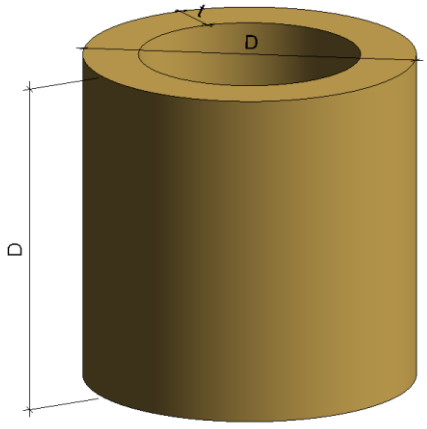

(c) UC specimen size

(d) UC test

Fig. 1. Specimen size and test. Note here that “U” indicates the grain direction, “T” indicates that tensile stress was applied, and “C” indicates that compression stress was applied

Tensile Test along the Grain

The size of the tensile specimen along the grain (UT) was 330 mm × 15 mm × *t* mm, and the length of 60 mm in the middle was the effective part of the specimen, as shown in Fig. 1a. When making the specimen, it is required that the texture is parallel to the center line, and the tangent direction of the green surface of bamboo should be perpendicular to the side of the effective part of the specimen. The transition arc surface between the effective part of the specimen and the clamping part at both ends should be smooth and symmetric with the center line of the specimen. Universal testing machine was used for loading at the rate of 0.01 mm/s (Fig. 1b).

Compression Test along the Grain

The size of the compressive specimen (UC) along the grain is *L*:*D*=1 (*L* is the height of the specimen), as shown in Fig. 1c. A universal testing machine was used to load at the rate of 0.01 mm/s (Fig. 1d). Lubricating oil was applied between the specimen and the loading section.

RESULTS AND DISCUSSION

Classification of Original Bamboo

Mechanical classification is based on the correlation between material strength and stiffness. According to the measured elastic modulus, the material grade boundary conditions are usually set, and then the material can be divided into different strength grades. The elastic modulus of bamboo is the basis of other mechanical properties. Based on the compression test, the distribution of the along-grain compression modulus (*UCE*) is shown in Fig. 2. The *UCE* of original bamboo conforms to Normal distribution and data distribution is relatively concentrated, mainly ranging from 12 to 15 GPa. Therefore, based on the stability of *UCE* distribution, *UCE* can be used as an index to evaluate other related mechanical properties in the performance evaluation system of original bamboo. Based on the above analysis, the mechanical classification grade limits of bamboo were set. The classification grades and their characteristic values are shown in Table 1.

In mechanical classification of original bamboo, the principle of classification is to divide bamboo resources into reasonable grades on the premise of meeting the requirements of use, so as to improve the comprehensive utilization value of bamboo. According to Table 1, bamboo could be divided into three grades I, II, and II by dividing different *UCE* intervals, and bamboo with grades II and III accounted for more than 80%. The coefficient of variation of *UCE* of original bamboo was less than 10%.

Table 1. Results of Bamboo Classification

Grade		Ⅰ	Ⅱ	Ⅲ
Grade Boundary (GPa)		﹤12	[12,15)	≥15
Proportion (%)		14.5	75.5	9.5
UCE	Mean	11.42	13.54	15.31
	5% quantile	10.95	12.1	15.05
	CV/%	2.7	6.37	1.67

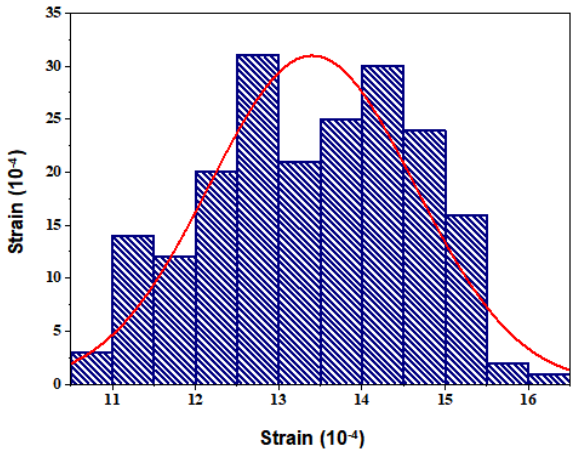

Fig. 2. *UCE* distribution

Analysis of Stress-Strain Curves

The tensile and compressive stress-strain curves of different grades of original bamboo along the grain are shown, respectively, in Fig. 3. As can be seen from Fig. 3, the tensile stress-strain curve of original bamboo along the grain presented roughly linear characteristics. The strain of original bamboo increased uniformly with the increase of stress. When the ultimate stress was reached, the specimen suddenly failed. That is, the failure mode of the tension along the grain of bamboo was brittle failure. The compressive stress-strain curve of original bamboo was obviously different from the tensile curve. With the increase of stress, the compressive stress-strain curve along the grain went through an elastic stage, an elastic-plastic stage, and a failure stage, successively. At the elastic stage, the relationship between stress and strain was linear. In the elastic-plastic stage, the stress-strain curve showed obvious nonlinear characteristics, such that the increase of strain increases gradually with the same increase of stress. According to the compressive stress-strain curve along the grain, the failure mode of bamboo along the grain compression was ductile failure.

Key Performance Indicators

Peak stress

Figure 4 shows the statistical results of peak stresses of the average stress-strain curves of the three grades along the grain tension and compression. As shown from Fig. 4, the peak stress increased gradually from grade I to grade III. The tensile peak stress of grade II along the grain was increased by 4.25% compared with grade I, and the peak stress of grade III was increased by 7.57% compared with grade II. The compressive peak stress of grade II along the grain is increased by 12.33% compared with grade I, and the peak stress of grade III was increased by 7.57% compared with grade II. Peak stress is very important for constitutive model. After the grading treatment in this paper, the peak stresses of the three grades of bamboo along the grain tensile strength and along the grain compressive strength showed gradient changes.

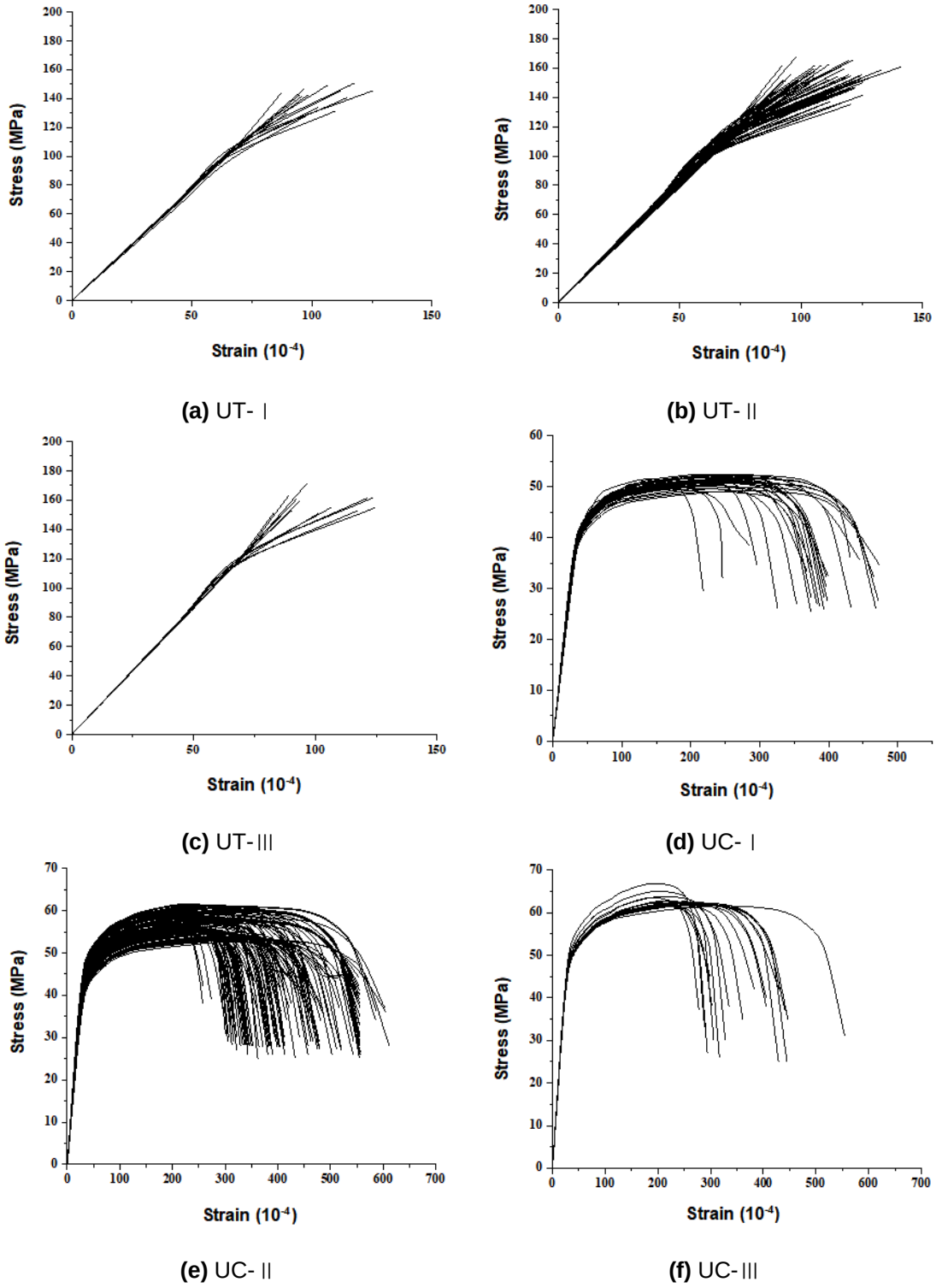

Fig. 3. Tensile and compressive stress-strain curves of original bamboo along the grain

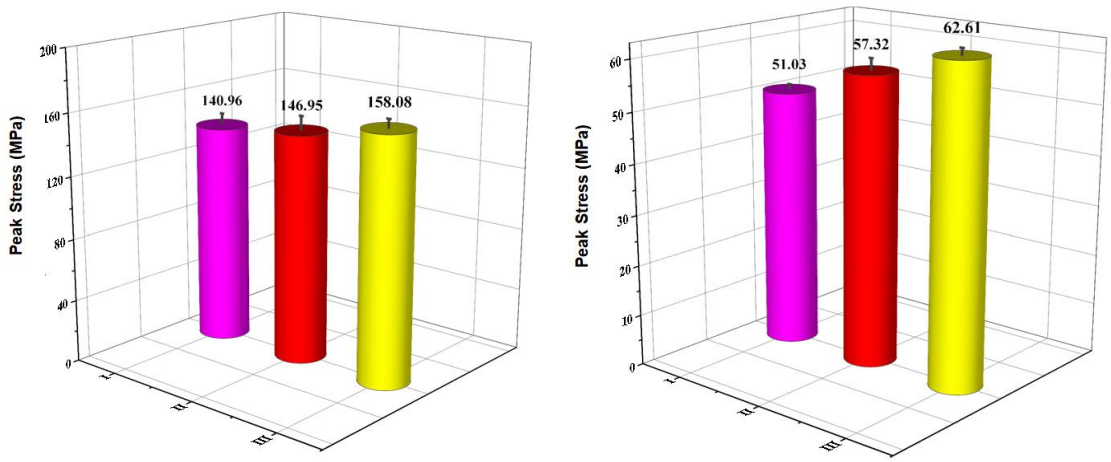

(a) UT **(b)** UC

Fig. 4. Peak stress statistics

Peak strain

The peak strain statistics of the average stress-strain curves of the three grades of tensile and compressive stress along the grain are shown in Fig. 5. The peak strains of tensile and compressive tensile along the grain were the largest at grade II. The fluctuation range of peak strain along grain tensile and compressive was 6.17% and 13.14%, respectively, which was smaller than that of peak stress. The results suggest that the peak strains of tensile and compressive along grain in the constitutive model should be represented by the average values of three grades, that is, the peak strains of tensile and compressive along grain are 0.0105 and 0.0238, respectively.

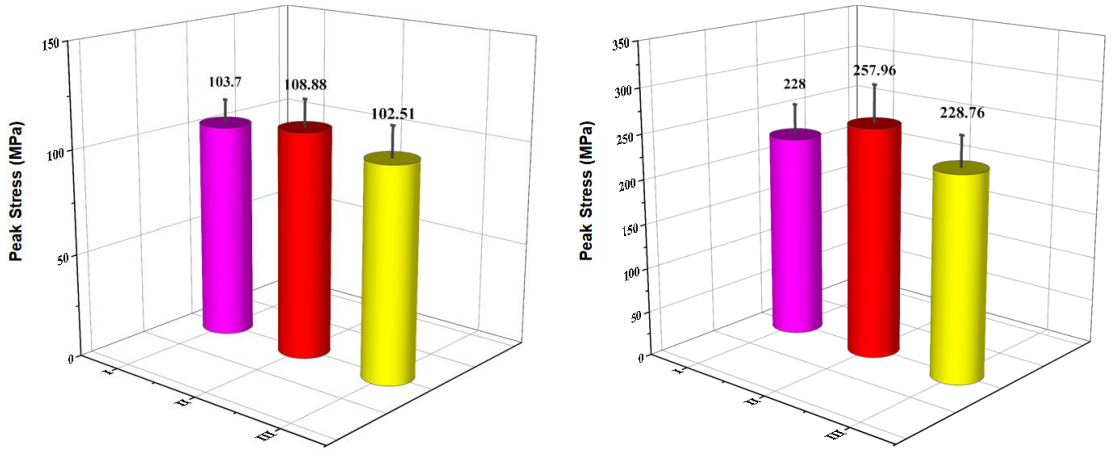

(a) UT **(b)** UC

Fig. 5. Peak strain statistics

Elastic modulus

Elastic modulus is an important parameter to characterize the slope of stress-strain curve, and also an important index to reflect the elasticity of materials. Figure 6 shows the statistics of elastic modulus of the average stress-strain curves of the three grades of tension and compression of original bamboo. The elastic modulus increased gradually from grade I to grade III. The tensile elastic modulus of grade II along the grain was increased by 11.14% compared with grade I, and the peak stress of grade III was increased by 0.99% compared with grade II. The compressive elastic modulus of grade II along the grain was increased by 18.56% compared with grade I, and the peak stress of grade III was increased by 13.07% compared with grade II.

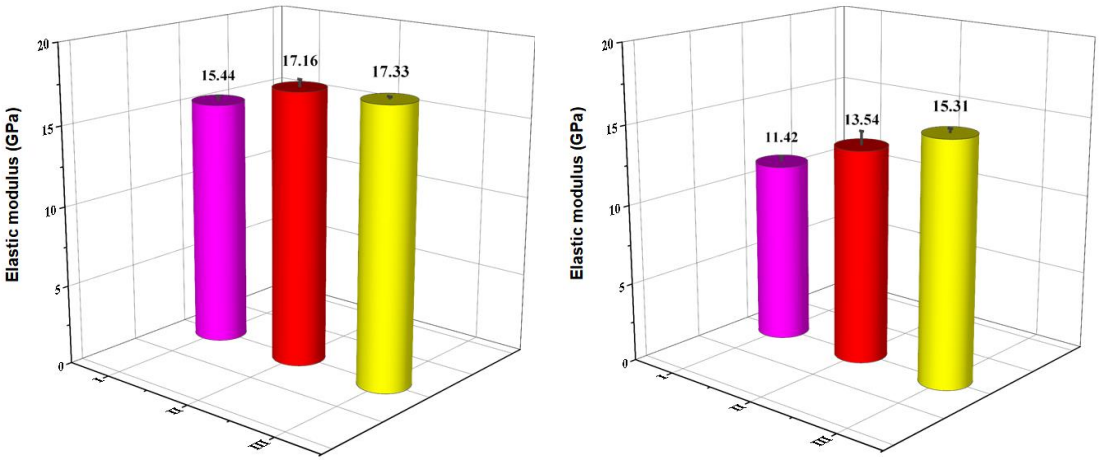

(a) UT **(b)** UC

Fig. 6. Statistics of elastic modulus

Constitutive models

Tensile constitutive model along the grain

As shown in Fig. 3, the tensile stress-strain curve of original bamboo presented linear elastic characteristics, so the linear relationship can be used to describe the tensile constitutive relationship of original bamboo along the grain, as shown in Eq. 1,

$$\sigma(\varepsilon)=E_t\varepsilon \quad (1)$$

where σ is stress (MPa), ε is strain, and E_t is tensile elastic modulus, MPa.

Simplified constitutive model for compression along the grain

The stress-strain curves were normalized, and the normalized stress-strain curves are shown in Fig. 7. The constitutive model of bamboo material was obtained from the average stress-strain curve of each grade. For the convenience of application, this paper proposes a simplified constitutive model, which is composed of three-segment polylines (Fig. 8). The first segment is the elastic segment, the second segment is the yield segment, and the third segment is the platform segment. In the elastic stage, the specimen retains its initial stiffness. At the yield stage, the stiffness of the specimen degenerates, and the displacement increases with the same increase of load. At the third stage the specimen is damaged.

The "three-fold line" constitutive model is shown in Eq. 2, and the key indicators of the "three-fold line" constitutive model at different grades are shown in Table 2.

$$\sigma(\varepsilon/\varepsilon_0)/\sigma_0=\begin{cases} m\varepsilon/\varepsilon_0 & 0\le\varepsilon/\varepsilon_0\le\varepsilon_y/\varepsilon_0 \\ \sigma_y/\sigma_0+km(\varepsilon/\varepsilon_0-\varepsilon_y/\varepsilon_0) & \varepsilon_y/\varepsilon_0<\varepsilon<1 \\ 1 & 1<\varepsilon<\varepsilon_u/\varepsilon_0 \end{cases} \quad (2)$$

$$k=\frac{1-\sigma_y/\sigma_0}{(1-\varepsilon_y/\varepsilon_0)m} \quad (3)$$

where σ is stress (MPa), ε is strain, m is the slope of elastic segment (MPa), σ_y is the proportional limit stress (MPa), σ_0 is the peak stress (MPa), ε_y is proportional limit strain, ε_0 is peak strain, ε_u is the maximum limit strain, and k is the slope coefficient of the nonlinear segment.

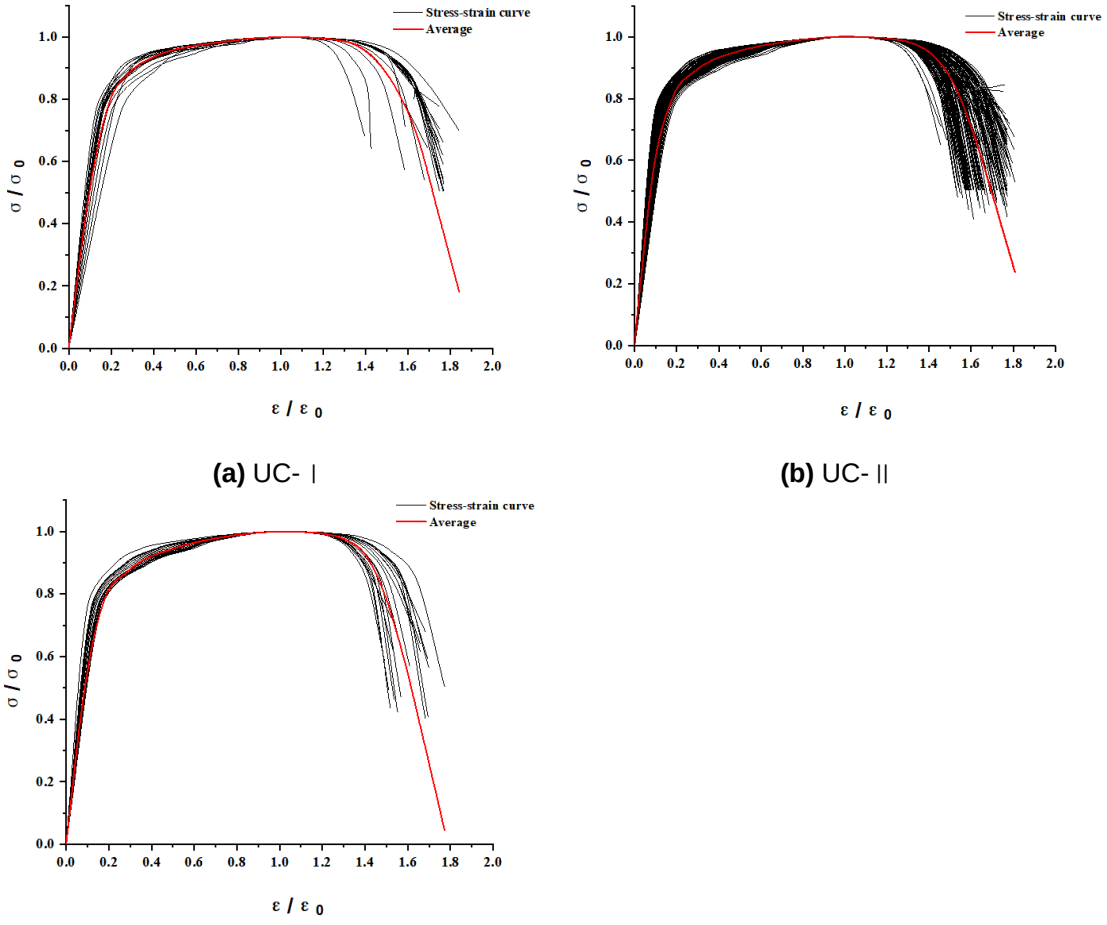

Fig. 7. Normalized stress-strain curves

Table 2. Parameters of Simplified Stress-strain Constitutive Model

	σ_y/σ_0	$\varepsilon_y/\varepsilon_0$	$\varepsilon_u/\varepsilon_0$
Grade Ⅰ	0.844	0.246	1.527
Grade Ⅱ	0.835	0.219	1.515
Grade Ⅲ	0.829	0.232	1.455

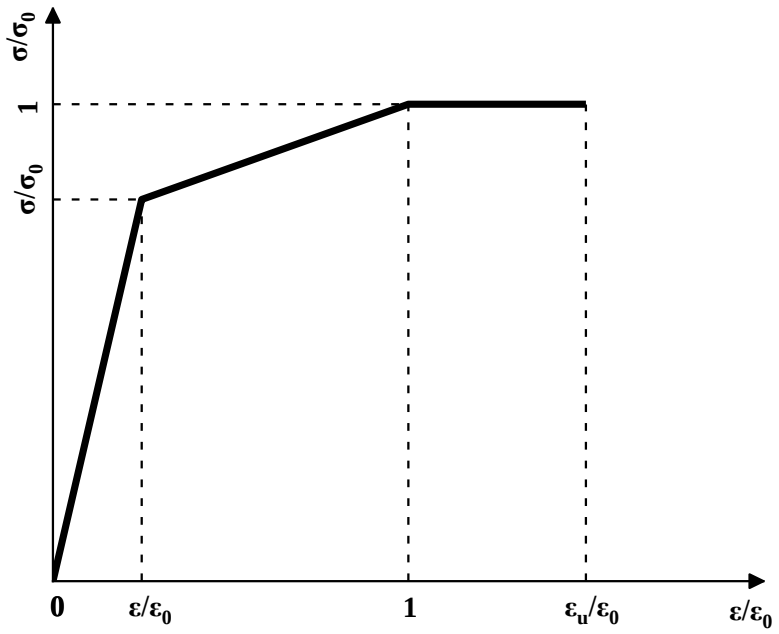

Fig. 8. Simplified stress-strain constitutive model

Accurate constitutive model of anti-compression along the grain

Table 3 shows the fitting results of constitutive models of average normalized stress-strain curves at different grades. Four typical models of ExpDec1, Bach, Sargin, and Tulin were selected for the constitutive model. The determination coefficients R^2 of the rising section fitted by the four constitutive models for stress-strain curves of different grades were all higher than 0.96, indicating that the four models were able to fit the rising section of stress-strain curves well. The determination coefficients R^2 of the four models for the descending section of stress-strain curves of different grades ranged from 0.535 to 0.987. The determination coefficients R^2 of Bach model was 0.535, and the fitting coefficients of the other three models were all higher than 0.92. The fit of the stress-strain curve with the Bach model was poor, so the Bach model was excluded first. The remaining models were used to fit the ascending and descending sections of the stress-strain curves.

The peak point is the key point of stress-strain curve, which should be paid special attention to when choosing constitutive model. In the ascending constitutive model, the peak point y fitted by ExpDec1 model and Bach model exhibited a certain negative deviation from the point (1,1), while Sargin and Tulin models were able to fit the peak point perfectly. Therefore, the Sargin and Tulin models can be considered to describe the ascending segment of the stress-strain curve. In the descending constitutive model, the peak

point of ExpDec1 model was higher than (1,1), while Sargin and Tulin models can fit the peak point perfectly. Therefore, the Sargin and Tulin models could be used to describe the descending section of the stress-strain curve. As the Tulin model parameter exhibited a large standard error in the descending phase, and the determination coefficient R^2 fitted by Sargin model was higher than Tulin model on the whole. The Sargin model is determined as the stress-strain constitutive model of original bamboo in this paper.

To compare the difference between the different parameters used in the rising section and the falling section and the uniform use of a set of parameters, this paper used the Sargin model to fit the complete stress-strain curve (including the ascending section and the descending section). The fitting results were obtained as shown in Table 4 and Fig. 9. The Sargin model achieved a high degree of agreement with the complete stress-strain curve. In order to make the constitutive model more concise and practical, a unified constitutive model was adopted in this paper to describe the stress-strain curve.

Table 3. Fitting Results of Stress-strain Constitutive Models

Model	Relationship Formula	Parameters		Parameter Values					
				Ⅰ		Ⅱ		Ⅲ	
				Ascent	Descent	Ascent	Descent	Ascent	Descent
ExpDec1		*a*	Values	-0.995	-2×10^{-4}	-9.757	-2.4×10^{-4}	-0.978	-3.6×10^{-4}
			Standard deviation	0.015	1.7×10^{-4}	0.018	2.3×10^{-4}	0.019	3.6×10^{-4}
		b	Values	0.131	-0.22	0.111	-0.222	0.123	-0.222
			Standard deviation	0.004	0.021	0.005	0.025	0.005	0.028
		c	Values	0.991	1.048	0.981	1.051	0.981	1.071
			Standard deviation	0.006	0.025	0.006	0.028	0.007	0.04
		R^2		0.998	0.99	0.997	0.987	0.996	0.984
		Peak point *y*		0.991	1.028	0.981	1.029	0.98	1.039
Bach		*a*	Values	1.051	1.184	1.04	1.171	1.047	1.202
			Standard deviation	0.032	0.166	0.023	0.147	0.027	0.19
		b	Values	0.207	-1.263	0.176	-1.234	0.201	-1.647
			Standard deviation	0.036	0.433	0.025	0.402	0.03	0.576
		R^2		0.95	0.522	0.973	0.55	0.964	0.533
		Peak point *y*		1.051	1.184	1.04	1.171	1.047	1.202
Sargin		*a*	Values	5.763	4.467	17.449	4.208	9.89	3.15
			Standard deviation	0.923	0.527	1.644	0.545	1.127	0.4
		b	Values	29.547	-1.384	-20.2	-1.27	7.243	-0.773
			Standard deviation	6.519	0.285	2.121	0.301	6.3	0.224
		R^2		0.998	0.984	0.988	0.982	0.996	0.981
		Peak point *y*		1	1	1	1	1	1
Tulin		*a*	Values	0.146	34.021	0.096	29.834	0.116	67.107
			Standard deviation	0.012	19.366	0.006	14.381	0.01	48.4
		b	Values	1.168	8.344	1.076	8.2	1.096	10.821
			Standard deviation	0.032	1.16	0.014	0.998	0.025	1.661
		R^2		0.996	0.911	0.999	0.93	0.997	0.92
		Peak point *y*		1	1	1	1	1	1

Table 4. Sargin Model Fitting Results of Complete Stress-strain Curve

Parameters		Parameter Values		
		Ⅰ	Ⅱ	Ⅲ
a	Values	7.896	9.028	6.568
	Standard deviation	0.999	1.34	1.099
b	Values	-3.253	-3.943	-2.709
	Standard deviation	0.534	0.729	0.608
R^2		0.953	0.938	0.912

Equation 4 is the constitutive model equation.

$$\sigma(\varepsilon)/\sigma_0=\frac{a\varepsilon/\varepsilon_0+(b\text{-}1)(\varepsilon/\varepsilon_0)^2}{1+(a\text{-}2)\varepsilon/\varepsilon_0+b(\varepsilon/\varepsilon_0)^2} \quad (4)$$

where σ_0 is peak stress (MPa), ε_0 is peak strain, and *a* and *b* are model parameters, as shown in Table 4.

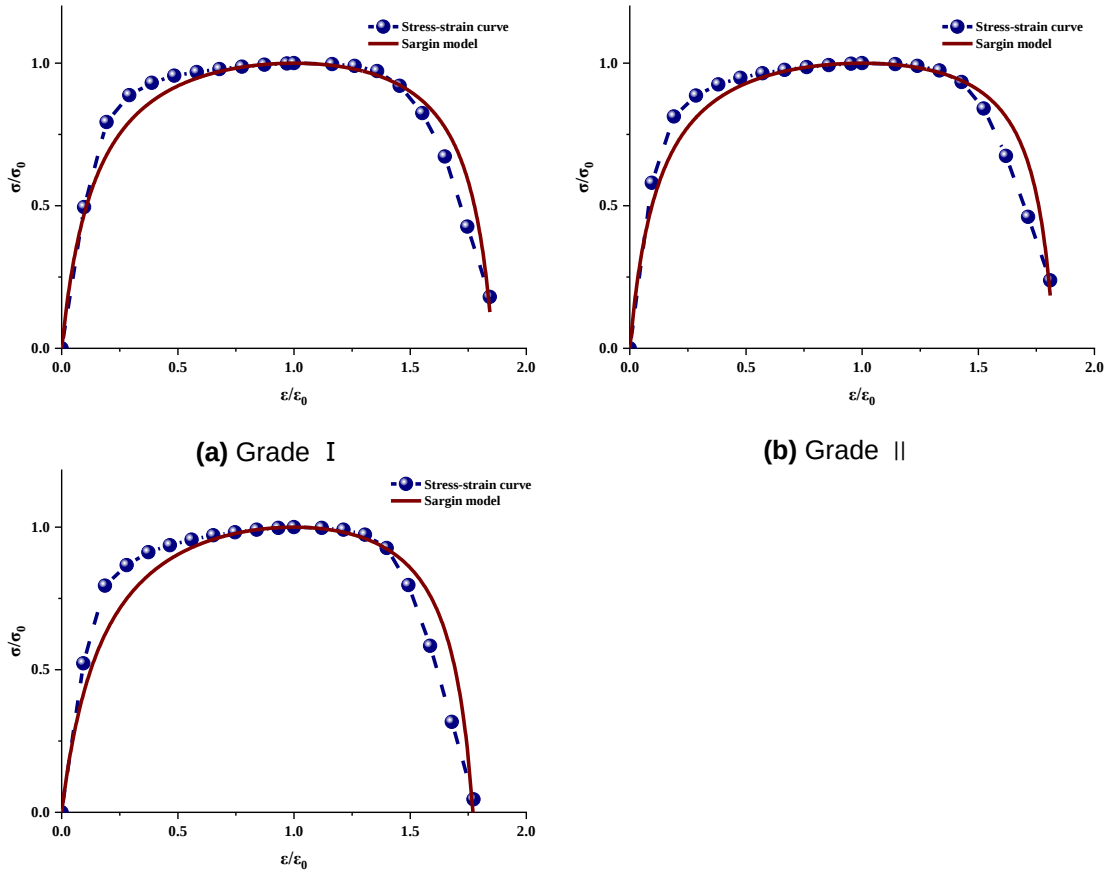

(a) Grade Ⅰ **(b)** Grade Ⅱ

(c) Grade Ⅲ

Fig. 9. Comparison of Sargin model curves and complete stress-strain curves

CONCLUSIONS

1. The tensile stress-strain curve of protobamboo along the grain showed linear elastic characteristics, and the failure mode was found to be brittle failure. The compressive stress-strain curve along the grain included an elastic section, an elastic-plastic section, and a failure section. The failure mode involved ductile failure.
2. The compressive elastic modulus of original bamboo along the grain was in accordance with the Normal distribution. The material was classified by the compressive elastic modulus of original bamboo along the grain, which could be divided into three grades. The elastic modulus less than 12 GPa corresponds to grade I, the elastic modulus of grade II is in the range of [12 to 15 GPa), and the elastic modulus not less than 15 GPa is grade III. The percentage of grade II and III was more than 80%.
3. The tensile constitutive model of original bamboo along the grain was found to adopt a linear relationship. A simplified constitutive model and an accurate constitutive model for grain compression based on gradation were proposed. The simplified constitutive model adopted a "three-fold" model, which can be easily used in calculation and analysis. By comparing four typical stress-strain constitutive models, the Sargin model was selected as the compressive stress-strain constitutive model of bamboo along the grain. Since there is no constitutive model of original bamboo, the stress-strain constitutive model of original bamboo based on gradation proposed in this paper is of great significance for the analysis of original bamboo structures.

ACKNOWLEDGMENTS

The authors are grateful for the support of the National Natural Science Foundation of China: [Grant Number 52204083].

REFERENCES CITED

Chen, F., Jiang, Z., Wang, G., and Cheng, H. (2012). "Mechanical properties of bamboo with diametric uniaxial and biaxial compression tests," *Journal of Shenzhen University Science and Engineering* 29(6), 527-533. DOI: 10.3724/sp.j.1249.2012.06527

Chen, Q., Zhang, R., Qin, D., Feng, Z., and Wang, Y. (2018). "Modification of the physical-mechanical properties of bamboo-plastic composites with bamboo charcoal after hydrothermal aging," *BioResources* 13(1), 1661-1677. DOI: 10.15376/biores.13.1.1661-1677

Fang, H., Sun, H., Liu, W., Wang, L., Bai, Y., and Hui, D. (2015). "Mechanical performance of innovative GFRP-bamboo-wood sandwich beams: Experimental and modelling investigation," *Composites Part B: Engineering* 79, 182-196. DOI: 10.1016/j.compositesb.2015.04.035

Huang, Z., Sun, Y., and Musso, F. (2017). "Assessment of bamboo application in building envelope by comparison with reference timber," *Construction and Building*

Materials 156, 844-860. DOI: 10.1016/j.conbuildmat.2017.09.026

ISO 22157–1. (2019). "Bamboo – Determination of physical and mechanical properties – Part I: Requirements," International Organization for Standardization, Geneva, Switzerland.

JG / T199-2007 (2007). "Test method for physical and mechanical properties of bamboo for construction," Ministry of Construction of the People's Republic of China, Beijing, China.

Jiang, Y., Nie, S., Liang, D., Zhang, N., Wang, S., and Song, X. (2015). "Effects of alkaline hydrogen peroxide pre-extraction on bamboo lignin chemistry and other bamboo chemical components," *BioResources* 10(4), 6332-6347. DOI: 10.15376/biores.10.4.6332-6347

Li, J., Yuan, Y., and Guan, X. (2016). "Assessing the environmental impacts of glued-laminated bamboo based on a life cycle assessment," *BioResources* 11(1), 1941-1950. DOI: 10.15376/biores.11.1.1941-1950

Li, H., Su, J., Zhang, Q., Deeks, A., and Hui, D. (2015). "Mechanical performance of laminated bamboo column under axial compression," *Composites Part B: Engineering* 79, 374-382. DOI: 10.1016/j.compositesb.2015.04.027

Li, H., Zhang, H., Qiu, Z., Su, J., Wei, D., Lorenzo, R., Yuan, C., Liu, H., and Zhou, C. (2020). "Mechanical properties and stress strain relationship models for bamboo scrimber," *Journal of Renewable Materials* 8(1), 13-27. DOI: 10.32604/jrm.2020.09341

Li, Z., Chen, C., Mi, R., Gan, W., Dai, J., Jiao, M., Xie, H., Yao, Y., Xiao, S., and Hu, L. (2020). "A strong, tough, and scalable structural material from fast-growing bamboo," *Advanced Materials* 32(10), article 1906308. DOI: 10.1002/adma.201906308

Liu, H., Jiang, Z., Zhang, X., Liu, X., and Sun, Z. (2014). "Effect of fiber on tensile properties of moso bamboo," *BioResources* 9(4), 6888-6898. DOI: 10.15376/biores.9.4.6888-6898

Liu, P., Xiang, P., Zhou, Q., Zhang, H., Tian, J., and Demis Argaw, M. (2021a). "Prediction of mechanical properties of structural bamboo and its relationship with growth parameters," *Journal of Renewable Materials* 9(12), 2223-2239. DOI: 10.32604/jrm.2021.015544.

Liu, P., Zhou, Q., Fu, F., and Li, W. (2021b). "Effect of bamboo nodes on the mechanical properties of *P. edulis* (*Phyllostachys edulis*) bamboo," *Forests* 12(10), 1309. DOI: 10.3390/f12101309

Liu, P., Zhou, Q., Zhang, H., and Tian, J. (2021c). "Design strengths of bamboo based on reliability analysis," *Wood Material Science & Engineering* 18(1), 222-232. DOI: 10.1080/17480272.2021.2014565

Lo, T., Cui, H., Tang, P., and Leung, H. (2008). "Strength analysis of bamboo by microscopic investigation of bamboo fibre," *Construction and Building Materials* 22(7), 1532-1535. DOI: 10.1016/j.conbuildmat.2007.03.031

Made Oka, G., Triwiyono, A., and Siswosukartoand Ali Awaludin, S. (2016). "Effects of bolt distance on flexural behavior of bolt-laminated bamboo beam," *International Journal of Engineering and Technology* 8(2), 112-116. DOI: 10.7763/ijet.2016.v8.868

Masood, S., and Khan, Z. (2017). "Adoption of green building technique: Replacement of steel by bamboo," *International Journal of Trend in Scientific Research and Development* 1(5), 452-457. DOI: 10.31142/ijtsrd2315

Mitch, D., Harries, K., and Sharma, B. (2010). "Characterization of splitting behavior of bamboo culms," *Journal of Materials in Civil Engineering* 22(11), 1195-1199. DOI: 10.1061/(asce)mt.1943-5533.0000120

Ni, L., Zhang, X., Liu, H., Sun, Z., Song, G., Yang, L., and Jiang, Z. (2016). "Manufacture and mechanical properties of glued bamboo laminates," *BioResources* 11(2), 4459-4471. DOI: 10.15376/biores.11.2.4459-4471

Nurazka, A., Pynkyawati, T., Davis, M., and Garnida, R. (2021). "Bamboo as a structure and construction material in the design of the bamboo Bukit Villa," *Journal of Architectural Research and Education* 3(1), 22-30. DOI: 10.17509/jare.v3i1.33943

Skuratov, S., Danilova-Volkovskaya, G., Yanukyan, E., and Beilin, M. (2021). "Bamboo as a unique ecological building material of the XXI century: Bamboo description, bamboo physical and mechanical properties studies," *Materials Science Forum* 1043, 149-154. DOI: 10.4028/www.scientific.net/msf.1043.149

Tian, L., Kou, Y., and Hao, J. (2018). "Flexural behavior of sprayed lightweight composite mortar-original bamboo composite beams: Experimental study," *BioResources* 14(1), 500-517. DOI: 10.15376/biores.14.1.500-517

Wang, Z., Li, H., Fei, B., Ashraf, M., Xiong, Z., Lorenzo, R., and Fang, C. (2021). "Axial compressive performance of laminated bamboo column with aramid fiber reinforced polymer," *Composite Structures* 258, article 113398. DOI: 10.1016/j.compstruct.2020.113398

Wei, Y., Zhou, M., Zhao, K., Zhao, K., and Li, G. (2020). "Stress–strain relationship model of glulam bamboo under axial loading," *Advanced Composites Letters* 29, 1-11. DOI: 10.1177/2633366x20958726

Zhao, W., Chen, Z., and Yang, B. (2017). "Axial compression performance of steel/bamboo composite column," *Procedia Engineering* 210, 18-23. DOI: 10.1016/j.proeng.2017.11.043

Zhou, Q., Xu, Y., Liu, P., Qin, Y., and Zhang, H. (2023). "Mechanical properties of energy sustainable round bamboo-phosphogypsum composite floor slabs," *Journal of Building Engineering* 76, article 107192. DOI: 10.1016/j.jobe.2023.107192

Zhou, X., Liu, P., Zhou, Q., Xiang, P., Zhang, H., and Tian, J. (2022). "Study on the tension and compression stress-strain relationship of *Phyllostachys edulis* bamboo parallel to the grain," *Industrial Crops and Products* 177, article 114548. DOI: 10.1016/j.indcrop.2022.114548

Article submitted: January 2, 2024; Peer review completed: February 22, 2024; Revised version received: February 26, 2024; Accepted: February 27, 2024; Published: March 26, 2024.
DOI: 10.15376/biores.19.2.3031-3046